On the seasonal circulation within the Panama Bight derived from satellite observations of wind, altimetry and sea surface temperature

Efraín Rodríguez-Rubio and Wolfgang Schneider

Departamento de Oceanografía, Universidad de Concepción, Chile
Centro de investigación Oceanográfica en el PAcífico Sur-oriental (COPAS), Universidad de Concepción, Chile

Rodrigo Abarca del Río

Departamento de Física de la Atmósfera y del Océano (DEFAO), Facultad de Ciencias Físicas y Matemáticas, Universidad de Concepción, Chile

Received 18 December 2002; accepted 14 March 2003; published 11 April 2003.

[1] The seasonal evolution of geostrophic currents in the Panama Bight is derived from satellite-borne altimeter data. Current literature describes the circulation in the Bight as being cyclonic only. Our study, instead, reveals two distinct seasonal patterns. In summer the circulation in the Panama Bight is anticyclonic, with a coastal current to the south, whereas in winter, the circulation reverses and is cyclonic with a coastal current to the north, and an oceanic upwelling center in the middle of the Bight. A seasonally changing wind field caused by the meridional migration of the Intertropical Convergence Zone, from 8–10°N in summer, to about 2°N in winter, controls the circulation of the basin. In summer southeasterly trade winds dominate the region, but in winte rnortheasterly trade winds of the North Atlantic, by means of the Panama Jet, enter the region via the Isthmus of Panama. *INDEX TERMS:* 4532 Oceanography: Physical: General circulation; 4512 Oceanography: Physical: Currents; 4279 Oceanography: General: Upwelling and convergences. **Citation:** Rodríguez-Rubio, E., W. Schneider, and R. Abarca del Río, On the seasonal circulation within the Panama Bight derived from satellite observations of wind, altimetry and sea surface temperature, *Geophys. Res. Lett.*, *30*(7), 1410, doi:10.1029/2002GL016794, 2003.

1. Introduction

[2] The Panama Bight is described as part of the eastern tropical Pacific Ocean delimited by the Isthmus of Panama (9°N) and Puntilla Santa Elena (2°S). It extends westward from the coasts of Panama, Colombia and Ecuador to about 81°W, and is subject to pronounced seasonal variations in oceanic conditions apparently related to changes in the position of the Intertropical convergence [e.g. *Kessler*, 2002]. At the same time, the region is also subject to strong interannual forcing associated with the El Niño-Southern Oscillation [*Fiedler et al.*, 1992; *Dewitte and Perigaud*, 1996].

[3] Interest in studying the oceanic and coastal oceanographic characteristics in the eastern tropical Pacific Ocean has increased since the 1950ies, when the international scientific community noticed its great productivity and its capacity in supporting important fish stocks like tuna and herring [*Wyrtki*, 1966]. Nevertheless, the Panama Bight only received little attention.

[4] Among the few oceanographic works published in International Journals, *Wooster* [1959] and *Bennett* [1965] described the general surface circulation of the Bight to be cyclonic. Eddy-like cyclonic features, during February and March, were observed in the northern Bight by *Stevenson* [1970] and *Andrade* [1992]. They connected them to regional upwelling scenarios. Recently, *Rodriguez-Rubio and Stuardo* [2002], investigated a phytoplankton bloom in the middle of the basin, during March 1997, related to oceanic upwelling introduced by the Panama Jet [*Chelton et al.*, 2000].

[5] The papers, cited above, highlight some important features of the Bight's general circulation patterns at various times of observation, whereas its seasonal cycle and mesoscale variability so far remains unknown owing of a lack of in-situ data. Here, we present a complete descriptive analysis of the spatial and temporal circulation within the Panama Bight based on satellite measurements of sea surface temperature, sea level anomalies and sea surface winds.

2. Data and Methods

[6] Sea surface temperatures (SST) were obtained from the Microwave Imager radiometer mounted on the Tropical Rainfall Measuring Mission satellite. The Microwave Imager operates at a frequency of 10.7 GHz, in which the atmosphere, including clouds, is nearly transparent, hence allowing a year round observation of sea surface temperatures with a spatial resolution of 0.25° in latitude and longitude. In this study, the weekly averaged SST product provided by Remote Sensing Systems, for the period December 1997 to December 2002, is used. Further details about the Microwave imager and its data processing are given by *Chelton et al.* [2001].

[7] Sea surface wind speed and wind direction stem from QuickScat, an acronym of the microwave scatterometer SeaWinds mounted on the QuickBird satellite. The spatial and temporal resolution is the same as for the Microwave Imager (0.25°, weekly). The data product was provided by Physical Oceanography Distributed Active Archive Center, and spans from July 1999 to December 2002. For further details refer to *Perry* [2001]. Wind stress is calculated according to *Smith* [1988].

[8] Gridded sea level anomalies (SLA), defined as the difference between the observed sea surface height and the

0094-8276/03/2002GL016794$05.00

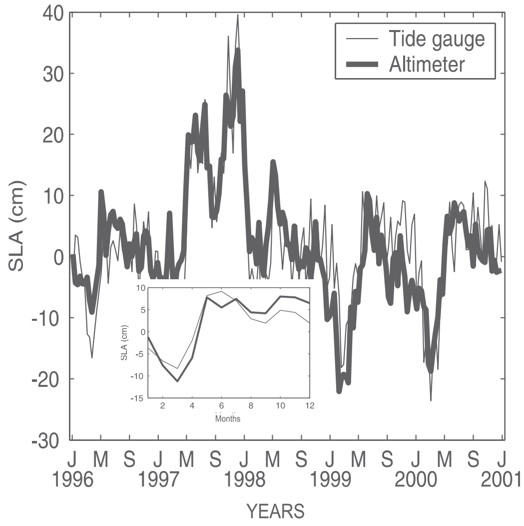

Figure 1. Comparison between SLA (thin solid line) from Buenaventura tide gauge (3°54.0 N, 77°06.0 W), and TOPEX/POSEIDON plus ERS1-2 (thick solid line), at 3°50.0 N, 77°15.0 W. The inlay shows the monthly climatologies for 5 years of data.

mean sea level, with a 0.25° resolution in latitude and longitude, provided every 10 days from January 1996 to August 2001, were obtained from the AVISO/Altimetry operations center. The product provided contains merged measurements from the altimeters mounted on board of TOPEX/POSEIDON and ERS 2 satellites to improve the map of mesoscale variability. Further details are given in *Ducet et al.* [2000]. Altimeter measurements coinciding with water depths less than 200 m were excluded in this study owing to potential problems, arising from not sufficiently accurate tidal models near the coast [*Le Provost*, 2001]. Geostrophic velocities were computed from sea level anomalies according to *Le Traon and Morrow* [2001].

[9] For sea surface temperature (January 1998 to December 2002), sea surface wind (July 1999 to June 2002), sea level anomaly and geostrophic current (August 1996 to July 2001), seasonal climatologies were computed, according to the seasonal cycle of the eastern tropical Pacific, i.e., January to March, April to June, July to September and October to December. In addition, in order to verify the validity of the seasonal cycle computed, we also calculated the climatologies for the period July, 1999 to June, 2001 only, which are covered by all three data bases, SST, sea surface wind and SLA, and no significant differences were found.

[10] A comparison of sea level height from the tide gauge at Buenaventura (Colombia), provided by the Instituto de Hidrología Meteorología y Estudios Ambientales (IDEAM), with the altimetry data showed a good agreement (Figure 1). From the tide gauge data a climatology for the years 1993 to 1996 was computed and subtracted from the sea level height in order to be consistent with the SLA product used here. The correlation between both time series (A 10-day average is used for the tide gauge data to match the AVISO SLA product) is r = 0.82, with a root mean square of rms = 6.0 cm. The correlation between the monthly climatologies resulted in r = 0.89, with rms = 4.48 cm, and the correlation between the seasonal climatologies in r = 0.91, with rms = 2.8 cm, and hence, justify the use of satellite sea level anomalies to calculate geostrophic currents in this study.

3. Results and Discussion

3.1. Sea Surface Temperature

[11] The most remarkable pattern in the distribution of SST is found in northern winter (January to March, Figure 2a). A cold plume of surface water, with temperatures ranging from 25.0°–26.5°C, stretches from the Gulf of Panama through the entire Bight in a south-southwesterly direction. Temperatures towards the west and the east of the plume rise by about 3°C. During spring, the plume retreats, showing an increase in SST in its central part. In summer (July to September, Figure 2b), the plume completely disappears. Instead, the northern part of the Bight warms by about 3°C, whereas the southern Bight slightly cools by 1°C. A new pattern of sea surface temperature distribution develops with increasing temperatures from the southwest to the northeast. In fall, the general shape of the isotherms is conserved; however, in the entire Bight, the temperatures drop by almost 1°C.

3.2. Sea Level Anomalies

[12] In northern winter, the pattern of sea level anomalies strongly resembles the SST distribution. The Panama Bight is dominated by a sea level low extending from the Gulf of Panama towards the south with a weak tendency towards the west (Figure 2c), and decreasing to the south. The SLA minimum (−11 cm) is centered slightly to the east of the SST minimum. Sea level rises toward the western boundary of our study region, where a positive signal around 6°N is noted. In spring the sea level low weakens, and in summer the situation reverses completely, showing an increase in sea level of 8 cm at the place of the wintertime negative anomaly (Figure 2d).

3.3. Geostrophic Circulation

[13] During the summer months, a single anticyclonic gyre, centered at about 5.5°N and 79.5°W, dominates the circulation pattern in the Panama Bight (Figure 1h). The maximal velocities, around 0.2 ms^{-1}, are found at the western and eastern slopes of the gyre, the former directed to the north around 82°W, and the latter to the south, forming a coastal southward current. In contrast, in winter, the Bight is controlled by an anticyclonic gyre in the west and a cyclonic gyre in the east (Figure 1g). Both gyres together, in the center of the Bight (81°W), contribute to, and form a strong southward current, exceeding 0.3 ms^{-1} in velocity and almost 200 km in width. The coastal current in the winter season, compared to summer is reversed, flowing northward.

3.4. Seasonal Oceanic Upwelling and Reversal in Circulation Forced by the Panama Jet

[14] The seasonally appearing cold tongue in the SST distribution within the center of the Bight, and the oscillation observed in the sea level anomalies can be explained by analyzing the seasonal wind field. The wind field of the Panama Bight is strongly influenced by the meridionally variable position of the Inter Tropical Convergence Zone (ITCZ) during the year. From June to September, the

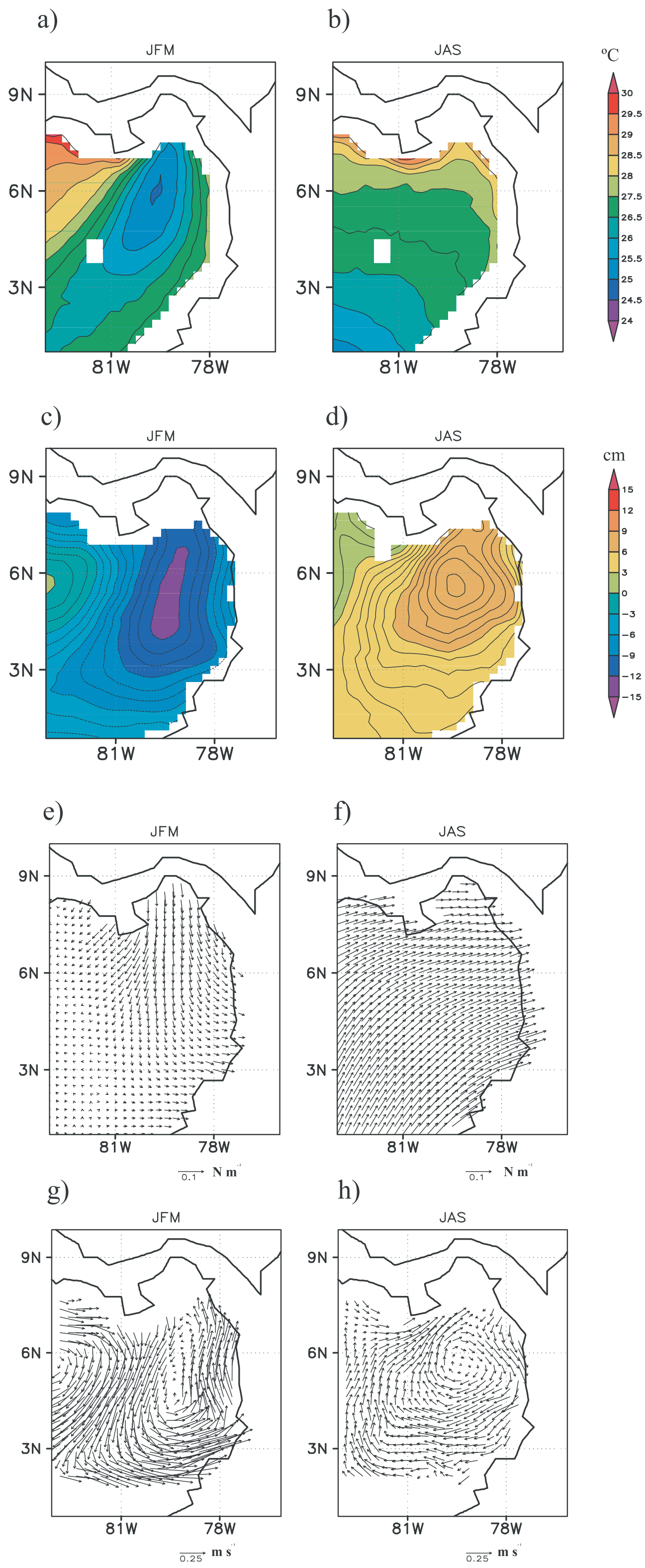

Figure 2. Annual cycle over the Panama Bight of SST JFM (a) and SST JAS (b); SLA JFM (c) and SLA JAS (d); Wind stress JMF (e) and wind stress JAS (f); and Geostrophic currents JFM (g) and geostrophic currents JAS (h).

ITCZ, in the eastern tropical Pacific, is positioned at around 8–10°N [*Forsbergh*, 1969; *Waliser and Gautier*, 1993], allowing the southeasterly trade winds of the Pacific to dominate the wind field in the Panama Bight. Once the trade winds cross the Equator in the Eastern Pacific, the change of sign of the Coriolis acceleration, land-sea temperature and friction gradients, force them into westerly directions [*Poveda and Mesa*, 2000]. The wind stress, for almost the entire study region, is on the order of 0.1 Nm^{-2}, with prevailing south-southwesterly and southwesterly directions (Figure 2f). In the northern portion of the Bight, the wind stress turns to westerly directions and diminishes in the Gulf of Panama, owing to its closeness to the Doldrums, related to the ITCZ. The prevailing wind field, together with the geometry of the Bight, result in an anticyclonic circulation with its center in the northeastern portion of the Bight (Figures 2d and 2h) and a southward flowing coastal current. The associated sea level high is enhanced by warming of the northern Bight during the summer months.

[15] Starting in October, the ITCZ moves southward, reaching its southernmost position in February and March [*Forsbergh*, 1969], which allows the northeasterly trade winds of the North Atlantic (Caribbean) to enter the region via the Isthmus of Panama, a physiographic gap of the mountainous topography of Central America. This local and temporally restricted high energetic wind event usually is referred to as the Panama Jet [*Chelton et al.*, 2000]. This jet, during winter, dominates the wind field of the northern Bight, which otherwise is shielded off from the northeasterly trade winds by the mountains of Central America. The wind stress in the Gulf of Panama exceeds 0.1 Nm^{-2}, with prevailing northerly directions (Figure 2e). The jet has a width of about 200 km, and extends for about 500 km into the Bight. At the western border of the jet winds turn anticyclonic to the west, whereas the southern Bight is in the doldrums beneath the ITCZ.

[16] Directly below the jet the coldest sea surface temperatures are found, with higher temperatures to the west (+4°C) and to the east (+2.5°C) of the main wind axis (Figures 2a and 2e). To the west of the jet an anticyclonic gyre (sea level high, downwelling), and to the east a cyclonic gyre (sea level low, upwelling) develop (Figures 2c and 2g). The observed SST distribution and the circulation pattern is explained by the model study of *McCreary et al.* [1989]. The authors investigated the response of the coastal ocean to strong offshore wind jets in the Gulf of Papagayo (West of Nicaragua and Costa Rica), similar in structure to the Panama jet, with a nonlinear 1 1/2-layer model that allows entrainment of cool water into the surface layer. As a result, cyclonic (east) and anticyclonic (west) gyres spinned up on either side of the jet due to Ekman pumping caused by wind stress curl, and entrainment of cool water lowers the SST along the axis of the jet. *Trasviña et al.* [1995] explored the offshore wind forcing in the Gulf of Tehuantepec, Mexico, a situation similar to the gulf of Panama, and found similar results, however, there the cyclonic gyre in the eastern part of the gulf was only weak.

[17] In summary, we have shown the existence of two distinct circulation patterns in the Panama Bight. These patterns are controlled by the reversing wind field. This coherent in-phase relation also is clearly confirmed by a complex Empirical Orthogonal Function analysis [*Horel*,

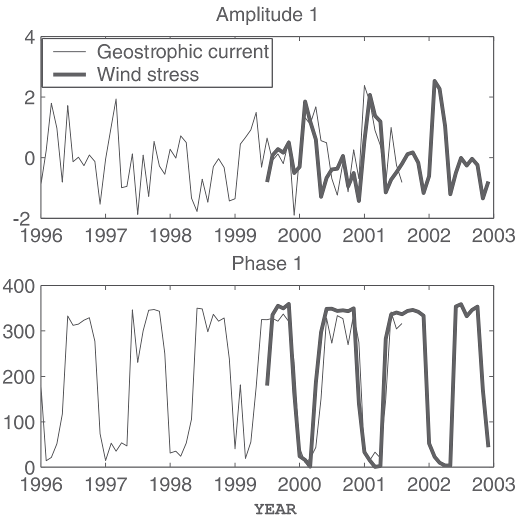

Figure 3. First mode of a Complex Empirical Orthogonal Function analysis of wind stress and geostrophic currents. The upper panel depicts the associated time series of normalized amplitudes and the lower panel the time series of the phases.

1984] of the winds and geostrophic currents (Figure 3). For wind stress and geostrophic currents, in the first mode, which explains 84% and 28% of the observed variance, respectively, two distinct states of phase exit, one between January and March, and the other one between May and November. The former phase, representing the occurrence of the Panama jet, is associated with high amplitudes in wind stress and geostrophic currents.

[18] **Acknowledgments.** This work was supported by the DAAD scholarship program, the research center COPAS of the Universidad de Concepción, Chile, the MECESUP scholarship program Chile, and IDEAM, Colombia. The altimeter products have been produced by the CLS Space Oceanography División as part of the European Union's Environment and Climate project AGORA (ENV4-CT9560113) and DUACS (ENV4-CT96-0357) with financial support from the CEO programme (Centre for Earth Observation) and Midi-Pyrenees regional council. CD ROMS are produced by the AVISO/Altimetry operations center.

References

Andrade, C. A., Movimiento geostrófico en el Pacífico Colombiano, *Bol. Cient. CIOH*, (12), 23–38, 1992.

Bennett, E. B., Currents observed in Panama Bay during September–October 1958, *Bull. Inter.-Am. Trop. Tuna Comm.*, *10*(7), 397–457, 1965.

Chelton, D. B., S. K. Esbensen, M. G. Schlax, N. Thum, M. H. Freilich, F. J. Wentz, C. L. Gentemann, M. J. McPhaden, and P. S. Schopf, Observations of coupling between surface wind stress and sea surface temperature in the Eastern Tropical Pacific, *J. Climate*, *14*, 1479–1498, 2001.

Chelton, D. B., M. H. Freilich, and S. K. Esbensen, Satellite observations of the wind jets off the Pacific Coast of Central America. Part II: Relationships and dynamical considetarions, *Mon. Wea. Rev.*, *128*, 2019–2043, 2000.

Dewitte, B., and C. Perigaud, El Niño-La Niña events simulated with Cane and Zebiak's model and observed with satellite or in situ data. Part II: Model forced with observations, *J. Climate*, *9*, 1188–1207, 1996.

Ducet, N., P. Y. L. Traon, and G. Reverdin, Global high-resolution mapping of the ocean circulation from TOPEX/Poseidon and ERS-1 and -2, *J. Geophys. Res.*, *105*(C8), 19,477–19,498, 2000.

Fiedler, P. C., F. P. Chavez, D. W. Behringer, and S. B. Reilly, Physical and biological effects of Los Niños in the eastern tropical Pacific, 1986–1989, *Deep-Sea. Res.*, *39*(2), 199–219, 1992.

Forsbergh, E. D., On the climatology, oceanography and fisheries of the Panama Bight, *Bull. Inter.-Am. Trop. Tuna Comm.*, *14*(2), 49–385, 1969.

Horel, J. D., Complex Principal Component Analysis: Theory and Examples, *J. Appl. Meteor.*, *23*(12), 1660–1673, 1984.

Kessler, W. S., Mean three-dimensional circulation in the Northeast Tropical Pacific, *J. Phys. Oceanogr.*, *32*, 2457–2471, 2002.

Le Provost, C., Ocean Tides, in *Satellite altimetry and earth sciences*, edited by L.-L. Fu and A. Cazenave, pp. 267–303, Academic Press, San Diego, 2001.

Le Traon, P. Y., and R. Morrow, Ocean currents and Eddies, in *Satellite altimetry and earth sciences*, edited by L.-L. Fu and A. Cazenave, pp. 171–215, Academic Press, San Diego, 2001.

McCreary, J. P., H. S. Lee, and D. B. Enfield, The response of the coastal ocean to strong offshore winds: With application to circulations in the Gulfs of Tehuantepec and Papagayo, *J. Mar. Res.*, *47*, 81–109, 1989.

Perry, K. L., *QuikSCAT science data product user's manual*, JPL, California, 2001.

Poveda, G., and O. J. Mesa, On the Existence of Lloró (the Rainiest Locality on Earth): Enhanced Ocean-Land-Atmosphere Interaction by a Low-Level Jet, *Geophys. Res. Lett.*, *27*, 1675–1678, 2000.

Rodriguez-Rubio, E., and J. Stuardo, Variability of photosynthetic pigments in the Colombian Pacific Ocean and its relationship with the wind field using ADEOS-I data, *Proc. Indian Acad. Sci. (Earth Planet. Sci.)*, *111*(3), 227–236, 2002.

Smith, S. D., Coefficients for sea surface wind stress, heat flux, and wind profiles as a function of wind speed and temperature, *J. Geophys. Res.*, *93*, 15,467–15,472, 1988.

Stevenson, M., Circulation in the Panama Bight, *J. Geophys. Res.*, *75*, 659–672, 1970.

Trasviña, A., E. D. Barton, J. Brown, H. S. Velez, P. M. Kosro, and R. L. Smith, Offshore wind forcing in the Gulf of Tehuantepec, Mexico: the asymmetric circulation, *J. Geophys. Res.*, *100*, 20,649–20,663, 1995.

Waliser, D. E., and C. Gautier, A satellite-derived climatology of the ITCZ, *J. Climate*, *6*, 2162–2174, 1993.

Wooster, W., Oceanographic observations in the Panama Bight,"ASKOY" expedition, 1941, *Bull. Am. Mus. Nat. Hist.*, *118*(3), 113–152, 1959.

Wyrtki, K., Oceanography of the Eastern Equatorial Pacific Ocean, in *Oceanogr. Mar. Biol. Ann. Rev.*, edited by H. Barnes, pp. 33–68, George Allen and Unwin Ltd., London, 1966.

R. Abarca del Río, Departamento de Física de la Atmósfera y del Océano (DEFAO), Facultad de Ciencias Físicas y Matemáticas, Universidad de Concepción, Barrio Universitario S/N, Concepción, Chile. (roabarca@udec.cl)

E. Rodríguez-Rubio and W. Schneider, Departamento de Oceanografía, Facultad de Ciencias Naturales y Oceanográficas, Universidad de Concepción, Barrio Universitario S/N, Cabina 5, Concepción, Chile. (erodrig@udec.cl; wschneid@udec.cl)